

Accepted Manuscript

Evaluation of the Bond Strengths Between Concrete and Reinforcement as a Function of Recycled Concrete Aggregate Replacement Level

Mahdi Arezoumandi, Amanda R. Steele, Jeffery S. Volz



PII: S2352-0124(18)30100-0
DOI: doi:[10.1016/j.istruc.2018.08.012](https://doi.org/10.1016/j.istruc.2018.08.012)
Reference: ISTRUC 321
To appear in: *Structures*
Received date: 19 July 2018
Revised date: 30 August 2018
Accepted date: 30 August 2018

Please cite this article as: Mahdi Arezoumandi, Amanda R. Steele, Jeffery S. Volz , Evaluation of the Bond Strengths Between Concrete and Reinforcement as a Function of Recycled Concrete Aggregate Replacement Level. Istruc (2018), doi:[10.1016/j.istruc.2018.08.012](https://doi.org/10.1016/j.istruc.2018.08.012)

This is a PDF file of an unedited manuscript that has been accepted for publication. As a service to our customers we are providing this early version of the manuscript. The manuscript will undergo copyediting, typesetting, and review of the resulting proof before it is published in its final form. Please note that during the production process errors may be discovered which could affect the content, and all legal disclaimers that apply to the journal pertain.

**Evaluation of the bond strengths between concrete and reinforcement as a
function of recycled concrete aggregate replacement level**

Mahdi Arezoumandi, Ph.D. (Corresponding author)

Assistant Professor, Department of Civil and Architectural Engineering, Shahab Danesh
University, Pardisan, Qom, Iran

Email: Arezoumandi@shahabdanesh.edu

Amanda R. Steele

Facilities Engineer, Chevron Energy Technology Company, 1400 Smith St., Houston, TX 77002,
USA

Phone: 713-372-5610

Email: amandaasteele@chevron.com

Jeffery S. Volz, Ph.D., P.E., S.E.

Associate Professor, School of Civil Engineering and Environmental Science, University of
Oklahoma, 423 Carson Engineering Center, 202 W. Boyd St., Norman, OK 73019-1024, USA

Phone: 405-325-1489, Fax: 405-325-4217

Email: volz@ou.edu

Abstract

The objective of this study was to determine the effect of replacing coarse natural aggregates for recycled concrete aggregates (RCA) on the bond strength between deformed mild reinforcing steel and surrounding concrete. Two different RCA replacement levels were considered, 50% and 100%, and were compared to a conventional concrete mixture.

To evaluate bond strength, 18 direct pull-out specimens were tested with both No. 13 and No. 19 reinforcing bars and nine full-scale beam specimens were tested with non-confined contact lap splices located at mid-span. Analysis of the test data indicates that replacing more than 50% of coarse natural aggregates results in diminished bond strength over concrete containing only virgin natural aggregates. This result suggests that the existing equation for development and splice length as reported in ACI 318 may require additional modification factors to account for the diminished bond strength when associated with replacement of coarse aggregates with RCA.

Keywords:

Recycled Concrete Aggregates, Conventional Concrete, Bond Strength, Pull out Specimens, Full Scale Beams Tests

1. Introduction

The construction of buildings, bridges, and roadways continues to increase in the twenty-first century, especially in areas with ever-growing populations. Existing structures and highways require repair or replacement as they reach the end of their useful service life or simply no longer satisfy their intended purpose due to the growing population. As modern construction continues, two pressing issues will become more apparent to societies: an increasing demand for construction materials, especially concrete aggregates, and an increasing production of construction and demolition waste. Already, the Federal Highway Administration (FHWA, 2004) estimates that two billion tons of new aggregate are produced each year in the United States. This demand is anticipated to increase to two and a half billion tons each year by 2020. With such a high demand for new aggregates, the concern arises of the depletion of the current sources of natural aggregates and the availability of new sources. Similarly, the construction waste produced in the United States is expected to increase. From building demolition alone, the annual production of construction waste is estimated to be 123 million tons (FHWA, 2004). Currently, this waste is most commonly disposed of in landfills.

To address both the concern of increasing demand for new aggregates and increasing production of waste material, many states have begun to recognize that a more sustainable solution exists in recycling demolished concrete for use as aggregate in new concrete as recycled concrete aggregates (RCA).

Many states in the USA have begun to implement recycled concrete aggregates in some ways in new construction. A small number of states in the USA (11 states) have begun using RCA in Portland cement concrete for pavement construction. The state of Missouri does not currently integrate RCA in any function (FHWA, 2004). Currently, there are no accepted standards or

guidelines in the United States for utilizing RCA in structural concrete, although in Europe there are several standards that regulate the use of RCA in concrete.

Concerns with concrete produced with RCA, often referred to as recycled aggregate concrete (RAC), involve the mortar which remains adhered to the surface of the RCA. In the production of RCA, the removal of all this residual mortar would prove costly and detrimental to the integrity of the virgin aggregates within the concrete. Therefore, residual mortar is inevitable. Research has shown that this residual mortar causes high water absorption, low density, low specific gravity, and high porosity in RCAs compared to natural aggregates (Kou et al. 2012). These effects in the recycled aggregate can decrease hardened concrete properties of RAC. According to Fathifazl et al. (2007), the amount of residual mortar on the RCA can significantly affect the mechanical and durability properties of RAC. To reduce the negative impacts of this residual mortar, new mix design methods such as the equivalent mortar volume method (EMV) can be used. However, it is worth mentioning that due to the presence of old attached mortar, the EMV method in many cases does not allow a 100% replacement ratio concrete to achieve the same properties of a reference ordinary concrete,. Additionally, further aggregate treatments and mixing methods, such as the Water Compensation Method or the Autogenous Self-Cleaning Method, are viable ways to improve RAC properties.

Due to the variety of sources of RCA and the various functions, environment, and wear of the concrete structures and pavements from which the RCA can be obtained, characterizing this aggregate can be very difficult. Controlled studies must be performed to account for each of these variables on a regional basis, such as for each state's department of transportation, so that the aggregates within the area can be adequately characterized.

Much of the existing literature on recycled concrete aggregates (RCA) focuses on the mechanical and durability characteristics of concretes made with RCA (Etxeberria et al., 2007; Gonçalves & de Brito, 2010; Kou & Poon, 2013). Relatively few studies have been conducted to evaluate the structural performance of RCA concrete (Corinaldesi & Moriconi, 2003; Pellegrino et al., 2013; Faleschini, & Pellegrino, 2013), and of those even fewer have concentrated on the bond characteristics of RCA concrete.

In a study by Ajdukiewicz and Kliszczewicz (2002), pull-out specimens designed per RILEM recommendations were used to evaluate bond performance of 0% and 100% RCA replacement. The mix designs used in this study were developed by conventional direct replacement of natural aggregates with RCA. They found that there is no significant difference between bond strength of deformed bars embedded in concrete with coarse RCA replacement and concrete containing only natural coarse aggregates. In this study, the greatest difference in bond strength was observed when smooth bars were used. There was a 20% decrease in bond strength when both coarse and fine aggregates were replaced with RCA, and an 8% decrease when natural sand and coarse RCA was used (Ajdukiewicz and Kliszczewicz, 2002). Typically, though, RCA fines are not recommended for use in new concretes.

Studies have shown that replacing natural sand with fine RCA will drastically increase the water demand and reduce the mix workability (ACI 555, 2001). Further studies have shown that the mechanical properties are more negatively impacted with the addition of RCA fines (Gonçalves & de Brito, 2010). The decrease in compressive strength, tensile strength, and modulus of elasticity are much more pronounced when both fine and coarse RCA are present than when only coarse RCA is present (ACI 555, 2001).

Xiao and Falkner (2005) investigated the bond performance of concretes with 0%, 50%, and 100% replacement of coarse natural aggregates only with RCA using 36 direct pull-out specimens. The conclusions from this study were similar to those by Ajdukiewicz and Kliszczewicz (2002), namely that no difference was observed between the bond strength of deformed bars at 0% RCA replacement and 50% or 100% RCA replacement. When smooth bars were used, a maximum decrease in bond strength of 12% was observed in the RCA concrete.

Generally, the mix design method used with RCA concrete has a significant impact on bond strength to mild steel reinforcing bars. Currently, there is no standard procedure for designing concrete mixtures containing RCA. The conventional method used in much of the current literature is a direct replacement of coarse aggregate with RCA. However, research has shown that the mortar attached to RCA negatively influences the mechanical and durability properties of RCA concrete (Shayan, 2003). To compensate for this residual mortar on RCA particles, Fathifazl (2008) has proposed a mix design procedure coined the “Equivalent Mortar Volume” (EMV) method. The key aspect of the EMV method is that the residual mortar of RCA is included in the total mortar volume of the mix, and the amount of new mortar and total amount of coarse aggregate are adjusted to account for this difference (Fathifazl, 2008). However, the EMV method negatively affects concrete workability (Etxeberria et al., 2007; Faleschini, & Pellegrino, 2013).

Existing research has shown that bond strength of RCA designed by the conventional method is lower than bond strength of RCA designed by the EMV method. In 2008, Fathifazl utilized beam-end test specimens to evaluate bond performance under a more realistic stress state response with both conventional and EMV mix designs. Using beam-end specimens with a Canadian standard No. 30 deformed reinforcing bars, Fathifazl found that the bond strength

(normalized by the square root of compressive strength) of concrete specimens designed using conventional methods of coarse aggregate replacement were 24% lower than their companion natural aggregate specimens. The study showed that bond strength of specimens designed using the EMV method were only 6% lower than their companion natural aggregate specimens.

(Fathifazl, 2008)

In order to investigate the effect of bar size, Fathifazl compared the bond strengths of beam-end specimens containing either a Canadian standard No. 16 or No. 30 deformed bar. RCA made from two different sources and with different original virgin aggregate material were used. He found that, regardless of the original virgin aggregate material in the RCA and mix design method, the specimens containing No. 16 bars had higher bond strengths than those containing No. 30 bars. These findings are in agreement with ACI 408 (2003) that the length to develop a reinforcing bar increases as bar diameter increases. This relationship is reflected in the development length equation presented in ACI 318 (2014). Furthermore, he found that when designed by the conventional method of direct replacement of natural aggregates for RCA, specimens containing No. 16 bars had 35% higher bond strengths than the specimens containing No. 30 bars. However, when designed by the EMV method, specimens containing No. 16 bars had bond strengths of at least 41% higher than those containing No. 30 bars (Fathifazl 2008).

In 2011, Butler et al. evaluated bond performance using 100% direct replacement of coarse aggregates with RCA using 24 beam-end test specimens. This study showed that natural aggregate beam-end specimens had bond strengths 9% to 21% higher than RCA beam-end specimens. Furthermore, they investigated a correlation between the RCA aggregate crushing value (ACV) and bond strength of concretes made with RCA. Using natural aggregates and two different sources of RCA, they found that as ACV increases, the bond strength decreases. For

both RCA sources, an ACV of the RCA was 26% to 43% higher than natural aggregates. This relationship was linked to the relationship to coarse aggregate crushing on fracture energy of concrete. Additionally, they observed a strong relationship between ACV and splitting tensile strength, namely that as ACV increases, splitting tensile strength decreases (Butler et al., 2011).

Breccolotti and Materazzi (2013) used mixes with 0%, 50%, 100% of recycled coarse aggregates to study the bond between the steel and concrete by pull out tests. Their test results showed that the normalized bond strength is only slightly affected by the replacement of normal aggregate with recycled aggregates.

Kim and Yun (2013 and 2014) investigated effect of aggregate size (20 and 25 mm), RCA replacement ratios (0%, 30%, 60%, and 100%), reinforcing bar directions (vertical and horizontal), and reinforcing bar locations on the bond behavior of deformed bars in RAC. Results of their study revealed that the RAC with lower aggregate size had a greater bond strength. In view of the top-bar effect, a significant difference was detected between the top and bottom bars at all ages. Furthermore, the predicted values of the bond stress from the ACI and CSA codes were significantly lower than those obtained from the experiment results. Regardless of the RCA replacement ratio, the RAC specimens showed a similar bond strength under the same age.

Prince and Singh (2013) tested 60 pullout tests with four different rebar diameters (12 mm, 16 mm, 20 mm and 25 mm) and four RCA replacement levels of 0%, 25%, 50%, 75% and 100%) to investigate the bond behavior of steel rebars in RCA concrete. They reported higher bond strength for the RCA concrete compared to the conventional concrete.

Similar study performed by Prince and Singh (2013) on 45 pullout specimens with 8, 10 and 12 mm diameter deformed steel bars concentrically embedded in recycled aggregate concrete designed using equivalent mix proportions with coarse RCA replacement levels of 25, 50, 75 and

100 %. All RCA replacement levels specimens showed higher bond strength compared with the natural coarse aggregate concrete specimens.

Prince and Singh (2014) studied bond performance of 30 pullout specimens (steel bars with 8 and 10 mm diameter and both normal and high-strength RCA with replacement levels of 25 %, 50 %, 75 % and 100 %). They observed that the normalized bond strength increased with an increase in the RCA replacement level.

Wardeh et al. (2017) reported results of 96 pullout specimens prepared with natural and RCA using 10 and 12 mm diameter deformed steel bars. Their specimens were fabricated with different incorporation ratios of fine and coarse recycled aggregates and only coarse recycled aggregates. Test results showed that for the same class of compressive strength the bond strength, bond-slip behavior and the associated failure mechanisms were very similar for the RCA and natural aggregate concrete specimens.

2. Research Significance

Based on a review of the existing literature, there are few studies that investigated the bond strength of reinforcing steel in RAC using full scale beam tests. The majority of studies have been performed exclusively through direct pull-out tests. Without this background, there is no quantitative basis for safely implementing RAC in structural design. Consequently, the authors, in conjunction with the Missouri Department of Transportation (MoDOT), developed a testing plan to evaluate structural performance of RAC specimens with local materials (Volz et al., 2014). The following research focuses on bond behavior of RAC specimens. The mix designs, based on standard mixes currently used by MoDOT, was on the lower end of cement content in order to develop a relatively harsh mix to investigate constructability issues common to RAC.

The experimental program, test results, and analyses for this study are presented in the following discussion.

3. Experimental Plan

The following section discusses details of mixture proportions, specimen design, test set up, and test procedure.

3.1. Materials and Mixture Proportions

For this study, three mix designs were produced and evaluated for bond performance. The mixture proportions and fresh properties of both the control concrete (CC) and RAC mixes are given in Tables 1 and 2, respectively. A Missouri Department of Transportation (MoDOT) Class B mix design served as the basis for the CC and RAC mixes. The specified amount of fine aggregate (natural sand from Missouri River Sand (Jefferson City, MO)) as a volume of total aggregates was 40%. Two RAC mixes were produced as modified MoDOT Class B mix designs. The direct replacement method of RCA for coarse aggregate (crushed limestone with a maximum nominal aggregate size of 25 mm from the Potosi quarry (Potosi, MO)) was used to design the RAC mixes. Two RCA replacement levels were considered: 50% (RAC-50) and 100% (RAC-100) volumetric replacement.

In order to control the number of variables in this experimental study, the recycled aggregates for the RAC mixes were produced by the researchers in a controlled laboratory environment. Unreinforced concrete beams were cast in five separate pours using the CC mix design. These beams were cured for a period of four months. At that point, the beams were taken to Capital Quarries (Rolla, MO) for production into recycled aggregate. Primary and secondary crushers reduced the concrete to the required size, which was then sieved to produce a MoDOT

D Gradation similar to the Potosi limestone used as the virgin aggregate. Aggregate test results for both the Potosi limestone virgin aggregate and RCA are shown in Table 3. The RCA has lower specific gravity and unit weight and much higher absorption. The LA abrasion test results were very similar.

All three concrete mix designs had a target compressive strength of 35 MPa and were batched and supplied by a local ready-mix concrete supplier. The RCA material was transported from Capital Quarries to the ready-mix plant and stored adjacent to the virgin limestone aggregate (recycled aggregates were pre-soaked prior to mixing). The purpose of using a local ready-mix plant to supply the concrete was to help transition the concept from the laboratory to the field.

Reinforcement for the test specimens consisted of ASTM A615 (2016), Grade 60 (414 MPa) steel. The results of mechanical property testing of the reinforcing steel are shown in Table 4. All of the reinforcing steel met the requirements for ASTM A615 and used the same deformation pattern. The 19 mm reinforcing bars had a relative rib area of 0.081.

3.2. Fabrication and Curing of Test Specimens

The bond test specimens and associated material property test specimens were fabricated and tested within the High Bay Research Laboratory at Missouri University of Science and Technology. All test specimens were moist cured for seven days using wet burlap and plastic sheeting. After the seven-day moist cure period, the specimens were removed from the formwork and allowed to cure within the controlled environment of the High Bay Research Laboratory, where the temperature and humidity were maintained between 18 to 24°C and 30 to 50% RH, respectively. All specimens were tested at an age of 28 days.

3.3. Pull-out Specimens

RILEM 7-II-128 RC6 (1994): Bond test for reinforcing steel describes the pull-out specimen as a steel reinforcing bar embedded in a concrete cube with a volume of $10d_s$ by $10d_s$ by $10d_s$, where d_s is the bar diameter. A direct tensile load is applied to the end of the steel bar until the bonded region fails. During testing, both the slip of the embedded bar and applied load are measured. The test specification calls for a bonded length of $5d_s$ and an un-bonded length of $5d_s$ at the end closest to the applied load. Some changes were made to the RILEM recommended test specimen design based on results from previous research (Arezoumandi et al., 2013).

The direct pull out specimen used in this experimental program was a reinforcing steel bar embedded in a cylindrical volume of concrete with a diameter of 30 cm (12 in.). This deviation from the RILEM standard was made to reduce the potential for a splitting failure by maintaining a constant, large concrete cover for the reinforcing bar. The bonded length was $5d_s$ and the un-bonded length was $5d_s$ as per the RILEM testing standard. This un-bonded length is necessary in the design of the direct pull-out specimens to prevent a conical failure surface from forming within the concrete volume at the location of bearing (ACI 408, 2003).

In this testing program, both ASTM A615 (2016), Grade 60 No. 13 (#4) and No. 19 (#6) deformed steel bars were used in direct pull out specimens. The total length of each bar measured 101.6 cm (40 in.). A length of 0.95 cm (3/8 in.) remained exposed at the end of the bonded portion to facilitate the measure of slip during testing using a linear voltage differential transformer (LVDT). The bonded and un-bonded lengths were 6.4 cm (2.5 in.) for the No.13 (#4) direct pull-out specimens and 9.5 cm (3.75 in.) for the No. 19 (#6) direct pull out specimens. A schematic of the No. 13 (#4) and No. 19 (#6) specimens are shown in Figure 1.

A 890-kN-capacity (200 kip) loading frame manufactured by Tinius Olson was used to test the direct pull out specimens. After the specimens were de-molded, they were inverted and positioned through the top platform of the load frame as shown in Figure 1. A steel bearing plate was used, and a neoprene pad was placed directly between the concrete surface and steel plate to ensure uniform bearing on the concrete. The steel bar was fed through grips on the middle platform of the testing frame. A smaller steel plate was placed on the top of the concrete cylinder and an LVDT was clamped to a magnetic stand at the top of the specimen. The head of the LVDT was placed on the 0.95 cm (3/8 in.) exposed end of the steel bar to measure the slip during testing. The LVDT set-up is shown in Figure 1.

The direct pull-out specimens were constructed to provide a relative measure of performance among the three mix designs. For this experimental program, a total of 18 pull-out specimens were tested. To investigate the effect of bar size on the relative bond performance, three specimens were constructed with No. 13 (#4) bars and three with No. 19 (#6) bars for each mix design.

Throughout the testing of these specimens, the slip of the bar and the applied load were recorded. When all testing was completed, the maximum applied load was determined for each pull-out specimen, and an average maximum value was found. The maximum bond stress was found by dividing the peak load carried by the bonded surface area of the bar.

3.4. Splice Beams

The beams (three for each mix design) used in this study were 3.05 m (10 ft.) long with a cross section of 30 cm x 46 cm (12 in. x 18 in.). The longitudinal reinforcement consisted of three ASTM A615 (2016), Grade 60 No. 19 (#6) deformed steel bars, which were contact lap-spliced at the midspan of the beams. The splice length used for these beams was a reduced value

of the development length equation recommended in ACI 318 (2014), shown as Equation 1. To ensure a bond failure occurs, the splice length was chosen as 70% of the development length (the splice length was chosen as 360 mm) calculated in accordance with Eq. 1.

$$l_d = \frac{3}{40} \frac{f_y}{\sqrt{f'_c}} \frac{\Psi_t \Psi_e \Psi_s}{\left(\frac{c_b + k_{tr}}{d_b} \right)} d_b \quad (1)$$

where:

l_d = the development length;

f_y = the specified yield strength of reinforcement;

λ = the lightweight concrete modification factor;

f'_c = the specified compressive strength of concrete;

Ψ_t = the reinforcement location modification factor;

Ψ_e = the reinforcement coating modification factor;

Ψ_s = the reinforcement size modification factor;

c_b = the smaller of the distance from center of a bar to nearest concrete surface and one-half the center-to-center spacing of bars being developed;

K_{tr} = the transverse reinforcement index,;

d_b = the nominal diameter of the reinforcing bar.

A standard hook was specified at the ends of each longitudinal reinforcing bar to achieve sufficient development. As per ACI 318 (2014), this hook included a 90-degree bend with the minimum recommended bend diameter of 11.4 cm (4.5 in.) and an extension of $12d_b$ at the free end of the bar.

Transverse reinforcement against shear failure consisted of No. 10 (#3), ASTM A615 (2016), Grade 60, U-shaped stirrups. To ensure that a shear failure would not occur before bond failure, a stirrup spacing less than the ACI 318 (2014) maximum stirrup spacing was used. The stirrups were not placed within the lap spliced region in order to avoid the interaction of confinement of the concrete within the splice zone. Figure 1 shows details of the cross-sectional and plan views of the beam splice specimens.

Four-point loading was used in order to create a constant maximum moment (and stress) in the middle third of the beam, helping to induce bond failure at the splice location at midspan. Figure 1 shows a schematic of the third-point loading condition used to test the beam splice specimens. The load frame consisted of two 490-kN, servo-hydraulic actuators and a series of spreader beams and rollers to apply the third-point loading. The test was performed in a displacement-controlled method at a rate of 0.5 mm/min.

Test instrumentation measured load, midspan deflection, and strain in the reinforcement at each end of the lap, as shown in Figure 1. After each loading step of approximately 22 kN, any cracking was traced in black markers to determine crack propagation. The beams were loaded until failure occurred, which was characterized by a very sudden rupture in the concrete along the bottom of the beam within the spliced region.

4. Test Results and Discussion

The following section discusses the results of pull-out, splice specimen tests and concrete mechanical properties for both the CC and RAC mixes.

4.1. Pull-out Specimens

Table 5 shows the results from the testing. All pull-out specimens failed in the same manner in which the reinforcing steel pulled out of the concrete cylinder without splitting the

concrete. In order to directly compare the test results, the values need to be normalized with respect to the compressive strength of each concrete type. In general, the majority of concrete design codes relate bond strength to the inverse square root of compressive strength (e.g., ACI 318 (2014), American Association of State Highway and Transportation Officials (AASHTO) Load and Resistance Factor Design (2017), Australian Standard 3600 (2009), Canadian Standards Association (2004), and Japan Society of Civil Engineers (2007)). However, ACI Committee 408 recommends an inverse fourth root relationship of bond strength to concrete compressive strength. Table 5 includes both a square root and fourth root normalization of the test data.

Based on the pull-out test results, the RAC specimens displayed higher bond strengths compared to the CC specimens for either normalization scheme. Applying the square root of compressive strength normalization indicated that the RAC-50 specimens achieved a 22 to 23% increase in bond strength over the CC specimens, while the fourth root normalization indicated a 19 to 20% increase. The RAC-100 specimens did not fare quite as well but still achieved a 3 to 8% increase in bond strength over the CC specimens based on the square root normalization and a 9 to 15% increase applying the fourth root normalization. A plot of the load-slip response as well as bond stress bar chart for each concrete type is shown in Figure 2. In general, all specimens displayed a very similar response with a significant linear portion up to approximately 70% of the failure load, followed by a slightly non-linear portion up to the peak load, and then an exponential decay in load with an accompanying significant increase in slip. Figure 2(b,c) clearly shows that the RAC 50 and CC had the highest and lowest normalized bond stress for both square and fourth root, respectively.

4.2. Splice Specimen Tests

4.2.1. Failure mode and Crack pattern

At failure, all of the beam splice specimens experienced a bond rupture/splitting failure. This failure was characterized by an abrupt audible and visible sign of splitting cracks parallel to the bars within the region of the splice. The load-deflection behavior is shown in Figure 3 for all three concrete types (average curves of each concrete type), which includes a steeper linear loading curve at the beginning of the test until the beam reaches flexural cracking, which is then followed by a shallower linear loading curve up to failure, which is characterized by a significant drop in load. Consistent with the linear load-deflection response, the reinforcing did not reach yield prior to failure based on the strain gages installed on each side of the splice. The cracking pattern for the specimens of each concrete type was also very consistent, as shown in Figure 4. Each specimen experienced vertical flexural cracking, particularly at the ends of the splice region, as well as horizontal cracking along the splice indicating a splitting type of failure.

Table 6 contains a summary of the longitudinal reinforcement stress at failure based on the strain gage readings. As noted previously, these values are taken from the strain gages installed at each end of each splice (see Figure 1). In general, the strain gage readings were very consistent for each specimen even accounting for localized cracking and the slight reduction in cross section necessary to install the instrumentation. These strains were then converted to stress using the stress-strain data measured for the reinforcing steel installed in the specimens. Unlike the pull-out specimens, the RAC specimens suffered a decrease in bond strength for the splice specimen tests. The RAC-50 splice specimens displayed a 9% and 29% lower average reinforcement stress at failure compared to the CC specimens for the square root and fourth root normalizations, respectively. The RAC-100 splice specimens displayed a 12% and 26% lower

average reinforcement stress at failure compared to the CC specimens for the square root and fourth root normalizations.

4.2.2. Material Properties Test Results and Comparison with Bond Strength

ACI Committee 408 (2003) has shown that several material properties of the concrete have a significant affect on the bond strength between mild reinforcing steel and the surrounding concrete, including splitting tensile strength, flexural strength, and fracture energy. These parameters have been shown to map well with the predicted failure response, particularly when the failure mode involves a splitting failure of the concrete within the zone of the lap splice. As a result, the following section investigates these parameters relative to the beam splice specimen test results.

Figure 5 shows a graphical comparison of the mechanical properties (Table 3) (splitting tensile strength, modulus of rupture and fracture energy) of the three mixes. These mechanical properties were determined from specimens fabricated from the same batches of concrete used in the construction of the pull-out and full-scale splice specimens. In order to compare the test results across mix designs, the splitting tensile strengths and moduli of rupture were normalized by dividing the test value by the square root of the concrete compressive strength. For fracture energy, the values were normalized by dividing the test value by the compressive strength raised to the power of 0.46. This method of normalization is based on Equations 2 and 3 from ACI 318 (2014) and Equation 4 from Bazant and Becq-Giraudon (2002):

$$f_{ct} = 6.7\sqrt{f'_c} \quad (2)$$

$$f_r = 7.5\sqrt{f'_c} \quad (3)$$

$$G_F = 2.5 \alpha_o \left(\frac{f_c'}{0.051} \right)^{0.46} \left(1 + \frac{d_a}{11.27} \right)^{0.22} \left(\frac{w}{c} \right)^{-0.30} \quad (\text{N/m}) \quad (4)$$

where $\alpha_o=1$ for rounded aggregate and 1.44 for crushed or angular aggregate.

As shown in Figure 5, all properties were negatively impacted with increasing replacement of coarse natural aggregates with RCA. The most drastic decreases were seen in splitting tensile strength and fracture energy. The splitting tensile strength decreased 14% and 25% for RAC-50 and RAC-100, respectively, and the fracture energy decreased 9% and 24% for RAC-50 and RAC-100, respectively. In bond failures where splitting cracks control, the peak load is governed by the tensile response of the concrete, which depends on its splitting tensile capacity and fracture energy. Thus, as shown in the deteriorated splitting tensile strength and fracture energy of high volume RCA concrete, it is expected that the bond carrying capacity will be negatively impacted. The modulus of rupture, f_r , decreased approximately 4% for RAC-50 and 8% for RAC-100.

These results show good agreement between mechanical properties (splitting tensile strength and fracture energy) and the splice specimen test results. It would appear that the cementitious matrix formed by the RAC results in lower mechanical properties than a conventional Portland cement matrix, leading to a corresponding decrease in bond strength.

4.2.3. Comparison of Test Results with Bond Test Database

Figure 6 contain a plot of the bond test database compiled by ACI Committee 408. The plot also contains the results of the nine, full-scale beam splice specimen tests performed in this study. Although there is considerable scatter in the bond test data, in general, as compressive strength increases, the bond strength increases. However, the results for the RAC specimens do not follow that trend. The RAC-50 specimens do have a lower bond strength than the CC

specimens with a corresponding lower concrete compressive strength. However, the RAC-100 specimens have a lower bond strength compared to the CC specimens yet a higher concrete compressive strength. It would appear that compressive strength is not the best predictor of bond strength for any of the database test results, particularly in the range of 20 to 40 MPa. Nonetheless, the plot does indicate the lower bond tests for both RAC mixes compared to the CC mix and that all the data is at least consistent with the database of previous bond test results.

5. Conclusions

To study the bond strength of reinforcing steel in RAC, 18 pull-out specimens as well as nine full-scale beam splice specimens were tested. Based on the results of this study, the following findings and conclusions are presented:

Pull-out Specimens:

The bond strength for the RAC-50 mix exceeded the CC mix by approximately 20%.

The bond strength for the RAC-100 mix exceeded the CC mix by approximately 10%.

All of the specimens had similar load-slip response.

All of the specimens failed by an adhesion failure or local crushing between the reinforcing steel ribs and the base concrete.

Beam Splice Specimens:

The bond stress-slip behavior for both the CC and RAC beam specimens was very similar, essentially linear until failure.

The cracking pattern for both the CC and RAC beam specimens was very similar, consisting of vertical flexural cracks at each end of the splice and horizontal splitting cracks along the splice region.

The bond strength for the CC mix exceeded the RAC-50 mix by approximately 10%.

The bond strength for the CC mix exceeded the RAC-100 mix by approximately 30%.

General:

The RAC mixes had enhanced bond strength with the reinforcing steel compared to the CC mixes when the failure did not result due to splitting, as evidenced by the pull-out specimens. However, when the failure was initiated by splitting of the concrete, the RAC mixes had lower bond strength compared to the CC mixes, as evidenced by the full-scale splice specimens.

There is very good agreement between the concrete mechanical properties (splitting tensile strength and fracture energy) and the full-scale splice specimen test results, primarily due to the splitting type of failure mode.

Acknowledgment

The authors wish to extend their sincere thank you to the Missouri Department of Transportation and the National University Transportation Center at Missouri University of Science and Technology. The conclusions and opinions expressed in this manuscript are those of the authors and do not necessarily reflect the official views or policies of the funding institutions.

References

Abbas, A., Fathifazl, G., Isgor, O. B., Razaqpur, A. G., Fournier, B., & Foo, S. (2007). Proposed method for determining the residual mortar content of recycled concrete aggregates. *Journal of ASTM International*, 5(1), 1-12.

Abbas, A., Fathifazl, G., (2008). Structural performance of steel reinforced recycled concrete members (Vol. 69, No. 02).

Ajdukiewicz, A., & Kliszczewicz, A. (2002). Influence of recycled aggregates on mechanical properties of HS/HPC. *Cement and concrete composites*, 24(2), 269-279.

American Association of State and Highway Transportation Officials (AASHTO) (2010). *AASHTO LRFD Bridge Design Specifications*, 4th Ed., Washington, D.C., USA.

American Concrete Institute ACI Committee (2014). “Building code requirements for structural concrete ACI 318-14 and commentary 318R-14.” ACI 318-14/318R-14, Farmington Hills, MI, USA: American Concrete Institute.

American Concrete Institute ACI 408. (2003). “Bond and Development of Straight Reinforcing Bars in Tension” (ACI 408R-03) Farmington Hills, MI, USA: American Concrete Institute.

American Concrete Institute ACI 555. (2001). “Removal and Reuse of Hardened Concrete” Farmington Hills, MI, USA: American Concrete Institute.

Arezoumandi, M., Wolfe, M. H., & Volz, J. S. (2013). A comparative study of the bond strength of reinforcing steel in high-volume fly ash concrete and conventional concrete. *Construction and Building Materials*, 40, 919-924.

AS 3600 (2009). "Concrete Structures," Standards Australia, Sydney, Australia.

ASTM C 39/C 39M (2012). "Standard Test Method for Compressive Strength of Cylindrical Concrete Specimens," ASTM, West Conshohocken, PA, USA, 7 pp.

ASTM C 78/C 78M (2010). "Standard Test Method for Flexural Strength of Concrete (Using Simple Beam with Third-Point Loading)" ASTM, West Conshohocken, PA, USA, 4 pp.

ASTM C 496/C 496M (2011). "Standard Test Method for Splitting Tensile Strength of Cylindrical Concrete," ASTM, West Conshohocken, PA, USA, 5 pp.

ASTM C 615/C 615M (2016). "Standard Specification for Deformed and Plain Carbon-Steel Bars for Concrete Reinforcement" ASTM, West Conshohocken, PA, USA, 8 pp.

Bazant, Z.P., and Becq-Giraudon, E. (2002) "Statistical prediction of fracture parameters of concrete and implications for choice of testing standards," *Cement and Concrete Research Journal*, V. 32, No. 4, pp. 529-556.

Breccolotti, M., & Materazzi, A. L. (2013). "Structural reliability of bonding between steel rebars and recycled aggregate concrete." *Construction and building materials*, 47, 927-934.

Butler, L., West, J. S., & Tighe, S. L. (2011). The effect of recycled concrete aggregate properties on the bond strength between RCA concrete and steel reinforcement. *Cement and Concrete Research*, 41(10), 1037-1049.

CSA CAN3-A23.3 (2004). “Design of Concrete Standards for Buildings,” Rexdale, Ontario, Canada.

Corinaldesi, V., & Moriconi, G. (2003). Recycled aggregate concrete under cyclic loading. In *Role of Concrete In Sustainable Development: Proceedings of the International Symposium dedicated to Professor Surendra Shah, Northwestern University, USA held on 3–4 September 2003 at the University of Dundee, Scotland, UK* (pp. 509-518). Thomas Telford Publishing.

Etxeberria, M., Mari, A. R., & Vázquez, E. (2007). “Recycled aggregate concrete as structural material.” *Materials and structures*, 40(5), 529-541.

Faleschini, F., & Pellegrino, C. (2013). Experimental behavior of reinforced concrete beams with electric arc furnace slag as recycled aggregate. *ACI Mater. J*, 110, 197-206.

Federal Highway Administration. (2004). *Transportation Application of Recycled Concrete Aggregate: Federal Highway Administration State of Practice National Review*, <<http://www.fhwa.dot.gov/pavement/recycling/applications.pdf>>

Gonçalves, P., & de Brito, J. (2010). “Recycled aggregate concrete (RAC)-comparative analysis of existing specifications.” *Magazine of Concrete Research*, 62(5), 339-346.

Japan Society of Civil Engineers (2007). "Standard Specification for Concrete Structure" JSCE No. 15, Tokyo, Japan.

Kim, S. W., & Yun, H. D. (2013). "Influence of recycled coarse aggregates on the bond behavior of deformed bars in concrete." *Engineering Structures*, 48, 133-143.

Kim, S. W., & Yun, H. D. (2014). "Evaluation of the bond behavior of steel reinforcing bars in recycled fine aggregate concrete." *Cement and Concrete Composites*, 46, 8-18.

Kou, S. C., & Poon, C. S. (2013). "Long-term mechanical and durability properties of recycled aggregate concrete prepared with the incorporation of fly ash." *Cement and Concrete Composites*, 37, 12-19.

Pellegrino, C., Cavagnis, P., Faleschini, F., & Brunelli, K. (2013). "Properties of concretes with black/oxidizing electric arc furnace slag aggregate." *Cement and Concrete Composites*, 37, 232-240.

Prince, M. J. R. and B. Singh (2013). "Bond behaviour of deformed steel bars embedded in recycled aggregate concrete." *Construction and Building Materials* 49: 852-862.

Prince, M. J. R. and B. Singh (2014). "Bond strength of deformed steel bars in high-strength recycled aggregate concrete." *Materials and Structures* 48(12): 3913-3928.

Prince, M. J. R. and B. Singh (2014). "Investigation of bond behaviour between recycled aggregate concrete and deformed steel bars." *Structural Concrete* 15(2): 154-168.

RILEM 7-II-128. (1994) "RC6: Bond Test for Reinforcing Steel. 1. Pull-Out Test." RILEM technical recommendations for the testing and use of construction materials, E & FN Spon, U.K., 102-105.

Shayan, A., & Xu, A. (2003). Performance and properties of structural concrete made with recycled concrete aggregate. *ACI Materials Journal-American Concrete Institute*, 100(5), 371-380.

Shi-Cong Kou, Chi-Sun Poon , Hui-Wen Wan, Properties of concrete prepared with low-grade recycled aggregates, *Construction and Building Materials* 36 (2012) 881–889.

Xiao, J., & Falkner, H. (2007). Bond behaviour between recycled aggregate concrete and steel rebars. *Construction and Building Materials*, 21(2), 395-401.

Wardeh, G., E. Ghorbel, et al. (2017). "Experimental and analytical study of bond behavior between recycled aggregate concrete and steel bars using a pullout test." *Structural Concrete* 18(5): 811-825.

List of Tables

Table 1- Mixture proportions of concrete

Table 2- Fresh and hardened properties of concrete

Table 3- Aggregate properties

Table 4- Mechanical properties of reinforcing steel

Table 5- Pull-out test results

Table 6 - Longitudinal steel reinforcement stress

List of Figures

Figure 1- Details of test specimens

Figure 2- Pull-out specimens test results

Figure 3- Load-deflections of the beam splice specimens

Figure 4- Crack pattern of the beams at bond failure

Figure 5- Change of mechanical properties of concrete (%)

Figure 6- Longitudinal steel reinforcement stress versus compressive strength of concrete

(database of ACI 408 (2003) and test results of this study)

Table 1- Mixture proportions of concrete

Material	Water kg/m ³	Cement kg/m ³	Fine aggregate kg/m ³	Coarse aggregate kg/m ³	Recycled Coarse aggregate kg/m ³	AE liter/m ³	HRWR liter/m ³
CC	126	315	745	1160	-	0.58	2.3
RAC-50	126	315	745	580	500	0.58	2.3
RAC-100	126	315	850	-	980	0.58	2.3

Table 2- Fresh and hardened concrete properties

Property	CC	RCA-50	RCA-100
Slump (mm)	180	155	140
Air content (%)	7	6	6.5
Unit weight (kg/m ³)	2380	2230	2150
Compressive strength ^{*1} (MPa)	27.6	24.5	33.3
Modulus of elasticity ^{*1} (GPa)	29.6	25.8	27.6
Flexural strength ^{*2} (MPa)	2.8	2.5	2.8
Splitting tensile strength ^{*1} (MPa)	2.7	2.2	2.2
Fracture energy ^{*3} (N/m)	265.7	229.2	220.5

¹: Values represent the average of three cylinders (ASTM C39-12, ASTM 469-14 and C496-11)

²: Values represent the average of three beams (ASTM C78-10)

³: Values represent the average of four notched beams (The beams measured 15×15×60 cm with a span length of 45 cm and notch with a depth of 3.8 cm and a thickness of 0.6 cm)

Table 3- Aggregate Properties

Property	CC	RCA
Bulk Specific Gravity, Oven-Dry	2.72	2.35
Dry-Rodded Unit Weight, (kg/m ³)	1600	1440
Absorption (%)	0.98	4.56
LA Abrasion (% Loss)	43	41

Table 4- Mechanical properties of reinforcing steel

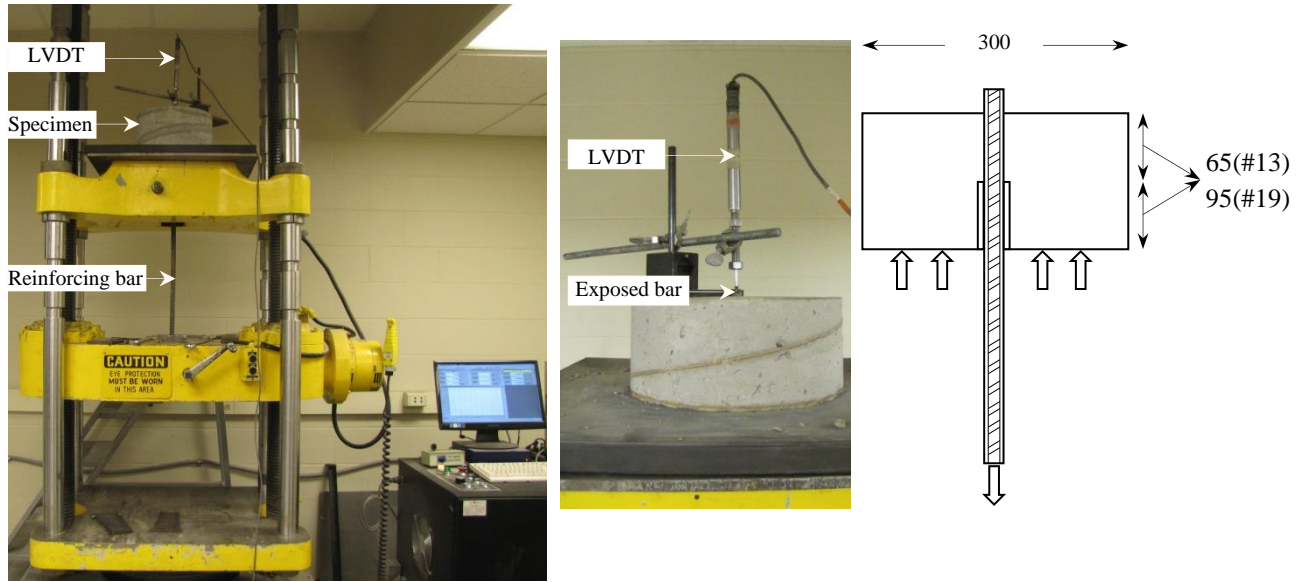
Bar No.	Yield Stress	Ultimate Stress	Modulus of Elasticity	Elongation
	(MPa)			(%)
13	510	698	196,570	13.3
19	494	675	192,180	15.4

Table 5- Pull-out test results

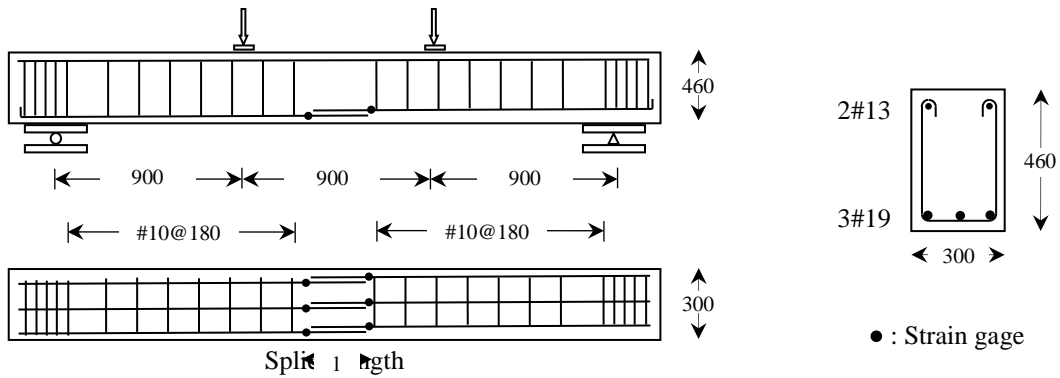
Section	f'_c (MPa)	Rebar size	τ (MPa)	τ_{ave} (MPa)	$\frac{\tau}{\sqrt{f'_c}}$	$\frac{\tau}{\sqrt[4]{f'_c}}$
CC	27.6	13	18.1	18.8	3.6	8.2
			18.3			
			20.0			
		19	21.2	20.4	3.9	8.9
			20.2			
			19.9			
RAC-50	24.5	13	22.4	21.9	4.4	9.8
			23.0			
			20.4			
		19	24.3	23.6	4.8	10.6
			22.2			
			24.5			
RAC-100	33.3	13	24.5	22.6	3.9	9.4
			21.5			
			21.8			
		19	23.6	23.3	4.0	9.7
			23.1			
			23.2			

Table 6 - Longitudinal steel reinforcement stress (MPa)

Section		f'_c (MPa)	f_s	$f_{s(ave)}$	$\frac{f_{s(ave)}}{\sqrt{f'_c}}$	$\frac{f_{s(ave)}}{\sqrt[4]{f'_c}}$
CC	1	27.6	434	450	85.7	196.3
	2		489			
	3		427			
RAC-50	1	24.5	393	384	77.6	172.6
	2		379			
	3		379			
RAC-100	1	33.3	325	350	60.7	145.7
	2		345			
	3		379			

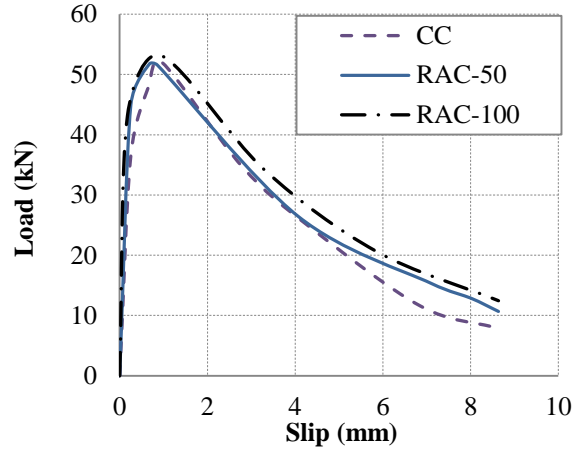


a) Direct pull-out specimen details and test setup

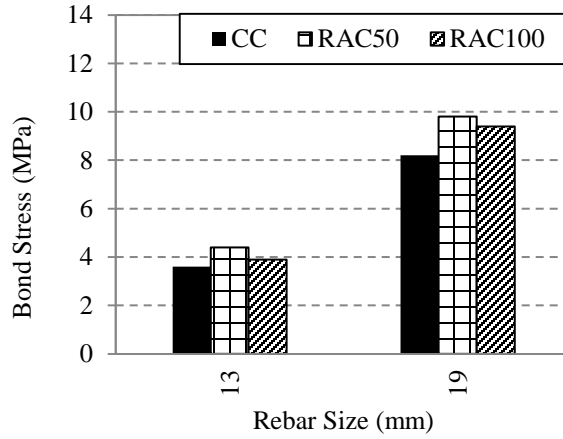


b) Splice specimen details

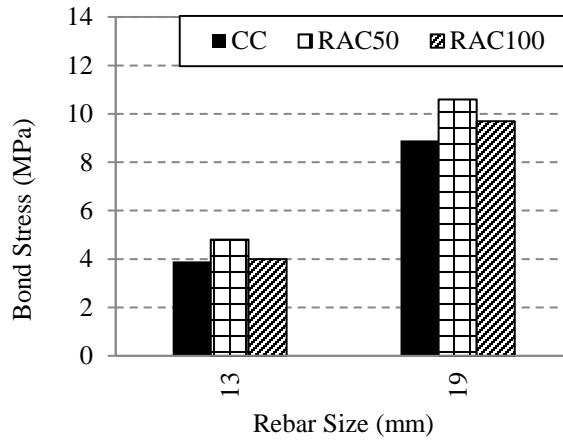
Figure 1- Details of test specimens
(All dimensions are in mm)



a) Load-slip plot



b) Bond stress plot (square root normalization)



c) Bond stress plot (forth root normalization)

Figure 2- Pull-out specimens test results

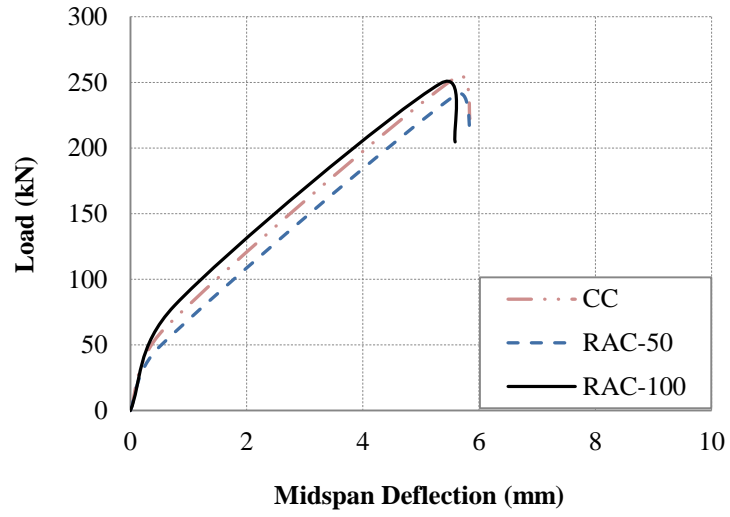


Figure 3- Load-deflections of the beam splice specimens

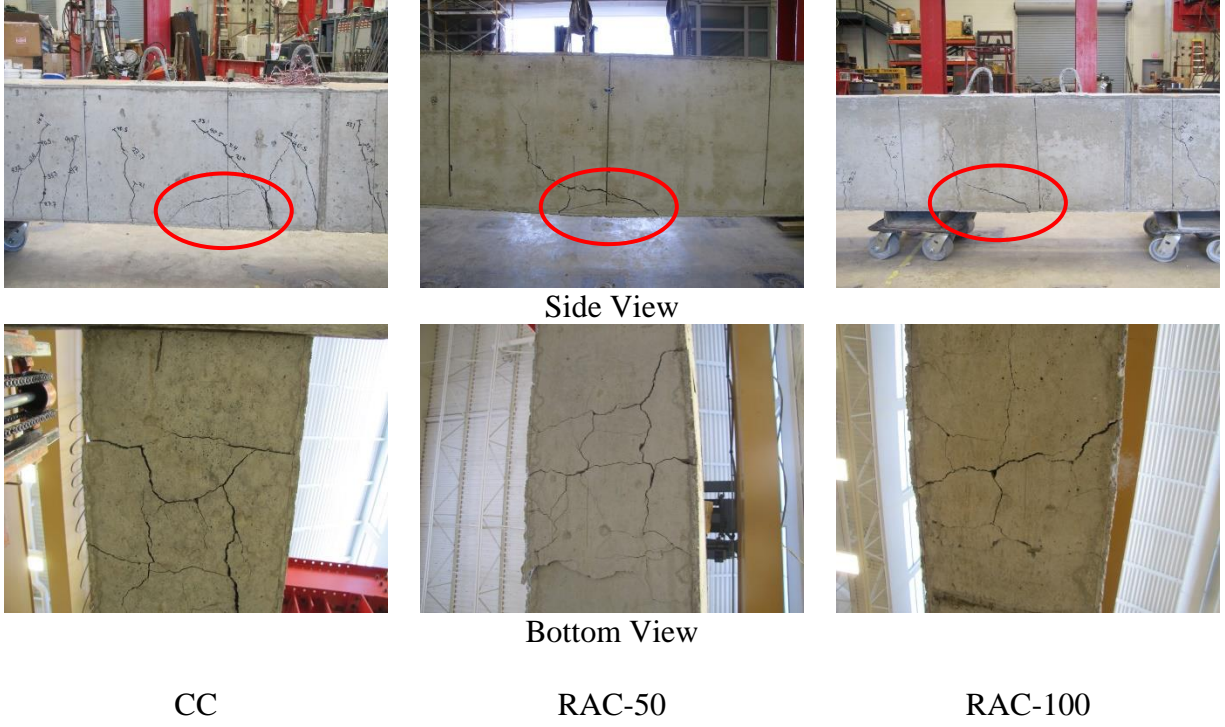


Figure 4- Crack pattern of the beams at bond failure

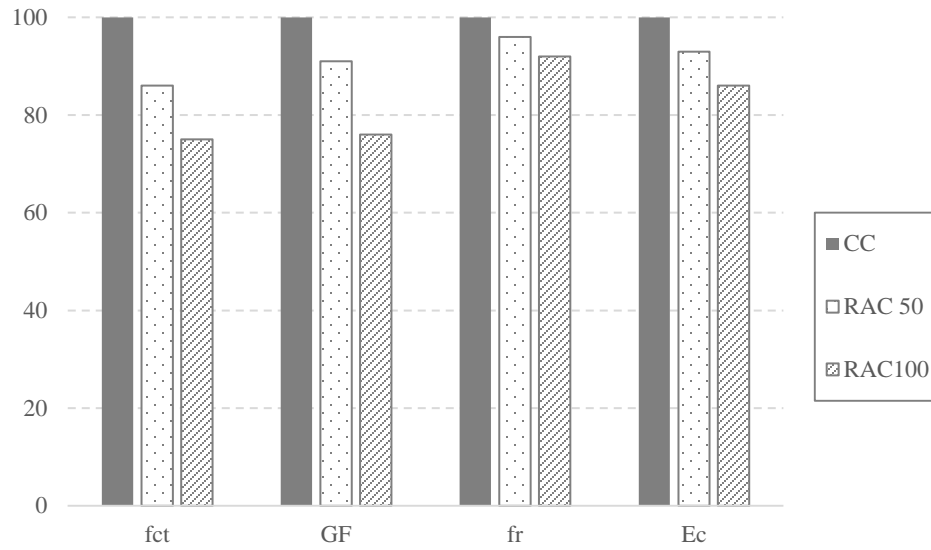


Figure 5- Change of mechanical properties of concrete (%)

f_{ct}: splitting tensile strength

G_F: fracture energy

f_r: modulus of rupture

E_c: modulus of elasticity

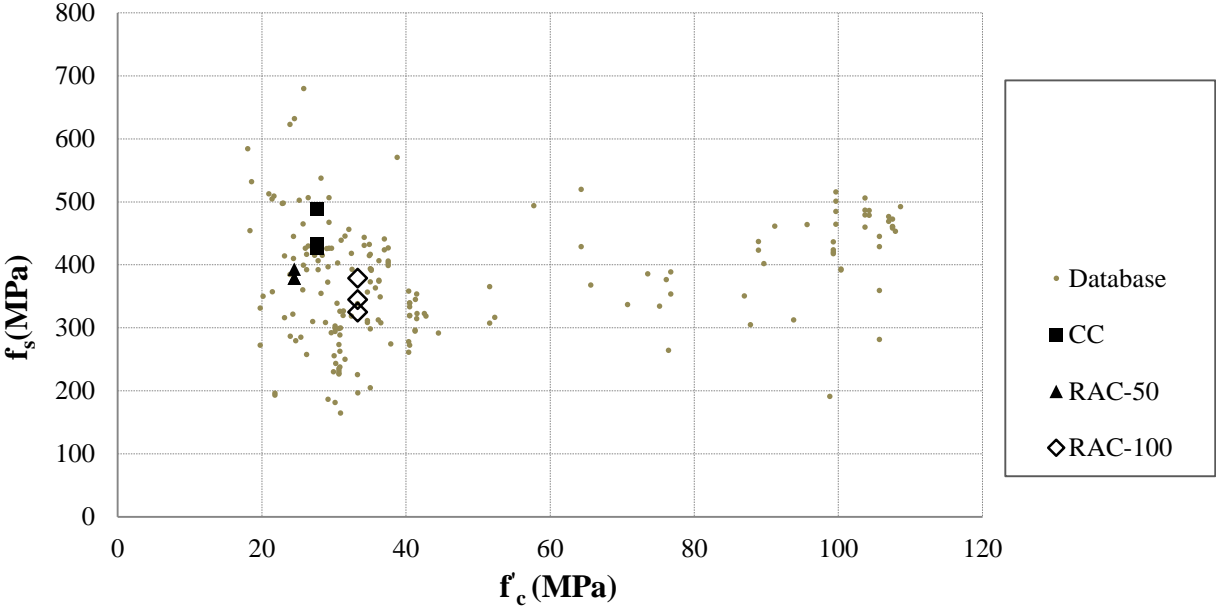


Figure 6- Longitudinal steel reinforcement stress versus compressive strength of concrete (database of ACI 408 (2003) and test results of this study)